Two Suboptimal Algorithms for Downlink Beamforming in FDD DS-CDMA Mobile Radio

Ying-Chang Liang, *Senior Member, IEEE,* and Francois Chin

***Abstract*—Two suboptimal algorithms are proposed for downlink beamforming in FDD DS-CDMA mobile radio by using uplink beamforming weights. One is a null-constrained method, which maintains the same null positions for both uplink and downlink beam patterns; the other is a frequency-calibrated method which constrains the same main beam positions for both patterns. We also evaluate the multicell downlink capacity of DS-CDMA systems using per-user-per-weight beamforming scheme. Outer cell interference is modeled as an AWGN process whose variance is proportional to the average intracell total tranmitted power. Computer simulations are given to compare the single cell and multicell capacities using different downlink beamforming weight generation algorithms.**

***Index Terms*—Adaptive beamforming, code division multiple access, frequency calibration, frequency division duplex, power control.**

I. Introduction

WIDEBAND DIRECT SEQUENCE code division multiple access (DS-CDMA) has been adopted as a radio access technology for third generation mobile communication systems due to its high system capacity and its flexibility to support a variety of voice and data services. The combination of spatial division multiple access (SDMA) and power control can provide improved capacity for DS-CDMA systems [1]–[4]. For example, maximal ratio combining (MRC) based weight generation and power-based power control are proposed in [1]; minimum mean squared error-based (MMSE) weight generation and signal-to-interference ratio-based (SIR) power control are proposed for CDMA without multidelay paths in [2] and with multidelay paths in [4]. In [10], we proposed a uplink beamforming and power control technique (UBPCT) to generate uplink beamforming weights for multirate CDMA with beamformer/Rake combiner two-stage structure. UBPCT, which takes care of multiple access interference (MAI) and interfinger interference (IFI) due to multidelay paths, generates uplink beamforming weights by minimizing all users' transmitted powers individually while maintaining the SIR requirement, thereby yields optimal solution in terms of power consumption as well as capacity enhancement.

In practice, it is also desirable to improve downlink performance; and in fact, downlink performance is even more important for the future communication systems in which wireless internet, video-on-demand and multimedia services are to be required. Traditional methods for downlink beamforming consist of two steps: 1) estimating instantaneous or statistical downlink channel responses and 2) computing downlink beamforming weights. So far, there are many literatures dealing with these two steps. Specifically, uplink and downlink channel responses are reciprocal for time-division-duplex (TDD) mode if the dwell time is small. For frequency-division-duplex (FDD) mode, however, both links use different carrier frequencies, thus the transmissions in these two links are independent. Therefore, probing-feedback approach is used to estimate instantaneous downlink channel responses [17]; or DOA-based approach [6], [16] or frequency-calibrated (FC) approach [12] is used to obtain statistical downlink channel responses. It is pointed out that the FC approach is a promising technique for estimating statistical downlink channel responses as it does not require to estimate DOAs.

If downlink channel responses are available, Rashid-Farrokhi *et al.* [4] proposed a virtual uplink beamforming and power control technique (V-UBPCT) to generate downlink beamforming weights by converting downlink beamforming problem into a virtual uplink problem. For CDMA systems, however, downlink beamforming problem does not correspond to a *solvable* virtual uplink one if MAI and IFI due to multi-delay paths are well considered. To solve this problem, Liang *et al.* proposed a modified V-UBPCT [11] by taking care of the IFI and MAI due to multidelay paths and orthogonality of downlink codes. In [11], we also considered multirate CDMA systems. The V-UBPCT method of [11] is based on the criterion of minimizing the total transmitted power while maintaining the SIR requirements, which is physically meaningful from the viewpoint of minimizing the interference pollution to the outer cells, thus of increasing the multicell capacity. From power control point of view, the downlink beamforming algorithms in [14] and [18]–[20], which are based on fixed transmitted powers, are not self-complete algorithms.

Even though much progress has been made for both steps in traditional downlink beamforming methods, we explore in this paper the possibility of generating downlink beamforming weights from a completely different way. In fact, since uplink beamforming weights are ready information at the base station, we try to generate downlink beamforming weights by modifying uplink ones for FDD DS-CDMA systems.

Let us compare the optimal solutions for uplink and downlink beamforming. Fig. 1 shows per-user-per-weight (PUPW) uplink beamforming scheme [10], with which the matched filter outputs for each path are passed to a beamformer, followed by a Rake combiner. The beamformer is used to track the DOAs, and average received powers of desired user and interfering

Manuscript received March 6, 2000; revised November 7, 2000.

The authors are with the Centre for Wireless Communications, Singapore Science Park II, Singapore 117674.

Publisher Item Identifier S 0733-8716(01)04709-6.

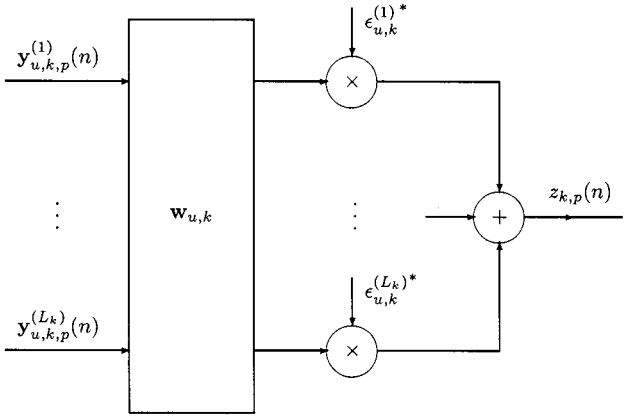

Fig. 1. PUPW uplink beamforming scheme.

users; while Rake combined is employed to maximize instantaneous signal-to-interference noise ratio (SINR). Since fast transmit power control is used in practice, the average powers for all users tend to be constant. Thus, the optimal uplink beamforming weights are dependent on the DOAs and constant received powers of all users. For downlink, a PUPW downlink beamformer is equipped at the base station [11], [15], and a normal Rake receiver is equipped at the mobile terminal. By converting downlink beamforming problem into a virtual uplink one, the optimal downlink beamforming weights are also functions of DOAs and constant *virtual* received powers of all users. It is seen that both optimal uplink and downlink beamforming weights are functions of DOAs of all users, which are the same for both links. Therefore, it is possible to generate downlink beamforming weights by modifying uplink weights for FDD systems. Two new methods are proposed: null constrained (NC) method, which maintains the same null positions for both uplink and downlink beam patterns; and frequency calibrated (FC) method, which constrains the same main beam positions for both beam patterns.

Since the optimal uplink and downlink weights are also functions of constant received powers in uplink and constant virtual received powers in downlink, which could be different for both links due to possibly asymmetric traffic, asynchronous reception and random codes/synchronous transmission and orthogonal codes in uplink/downlink, the optimal downlink beamforming weights could not be generated from uplink weights completely. Therefore, the new algorithms are referred to as suboptimal methods. However, compared with the optimal solution which requires complicated computations, the new algorithms are simpler for implementation.

Another objective of this paper is to propose a method for evaluating multicell capacity of a multirate DS-CDMA system with base station antenna array using joint beamforming and power control technique. Outer cell interference is modeled as an additive white Gaussian noise (AWGN) process whose variance is proportional to the average intracell total tranmitted power. A new simple method is proposed for evaluating downlink multicell capacity. With the new method, it is able to compare different downlink beamforming algorithms.

This paper is organized as follows. In Section II, the uplink and downlink system models are given. Section III studies uplink beamforming and power control problem in which single cell and multiple cell cases are considered. In Section IV, single cell and multiple cell downlink capacities are considered by using downlink beamforming and power control technique. Section V compares real and virtual UBPCTs, and propose two suboptimal algorithms for generating downlink beamforming weights. Computer simulation results are given in Section VI to evaluate the multicell capacities for different downlink beamforming algorithms. Finally, conclusions are drawn in Section VII.

II. System Description

Suppose N mobile users share the same sector in which a M-element uniform linear array (ULA) is equipped. Narrowband signals are first spread to wideband signals using different spreading codes, then transmitted to the desired user. For uplink, signals received at base station antenna array are passed into an adaptive beamformer, followed by a Rake receiver for coherent detection. For downlink, signals to be transmitted are first multiplexed at the base station antenna array, then transmitted through physical channels; while at mobile terminals, Rake receivers are employed in order to coherently detect the information signal.

A. Uplink and Downlink Signal Spreading

In uplink, only long random spreading is used for basic data rate users; while for high data rate users, the data sequences are first converted to several parallel basic rate data streams, with each of them spread by different orthogonal short spreading sequences and then summed up to be randomized by a long random sequence with the same chip rate as the basic rate users. Specifically, suppose user k is with normalized data rate $r_u(k)$, which is the ratio of the kth user's uplink data rate to the basic data rate. If $r_u(k) \neq 1$, the kth received signal at the base station is $s_{u,k}(t) = \sqrt{P_{u,k}} \sum_{j=1}^{r_u(k)} \tilde{d}_{u,k}^{(j)}(t)\tilde{c}_{u,k}^{(j)}(t)$, where $\tilde{d}_{u,k}^{(j)}(t)$ and $\tilde{c}_{u,k}^{(j)}(t)$ are the data signal and spreading signal, respectively; $P_{u,k}$ the average received power for one code channel of user k. The basic processing gain is G.

In downlink, the basic data rate users are first spread by different orthogonal short spreading codes, and then summed up to be randomized by the same long random sequence with the same chip rate as the orthogonal spreading sequences. For high data rate users, the data sequences are first converted to several parallel basic rate data streams, with each of which spread by different orthogonal short spreading sequences and then summed up to be randomized by the long scrambling sequence.

Suppose user k is with normalized data rate $r_d(k)$, which is the ratio of the kth user's downlink data rate to the basic data rate. Let $\tilde{d}_{d,k}^{(j)}(t)$ and $\tilde{c}_{d,k}^{(j)}(t)$ be the data signal and spreading signal of the kth user's jth code channel, respectively, and $P_{d,k}$ the average transmitted signal power for one code channel of user k. The kth signal to be transmitted to mobile user k is $s_{d,k}(t) = \sqrt{P_{d,k}} \sum_{j=1}^{r_d(k)} \tilde{d}_{d,k}^{(j)}(t)\tilde{c}_{d,k}^{(j)}(t)$, for $k = 1, \ldots, N$.

B. Channel Models

A discrete time delay wide sense stationary uncorrelated scattering (WSSUS) model is employed to represent the

channel [7], [13]. Specifically, due to reflections by obstacles, many propagation paths with different time delays are created. A DS-CDMA receiver resolves the multipath into several delay paths having discrete time delays which equal to the multiples of the spreading sequence chip duration T_c. The resolved delay path with time delay τ represents a group of multipath components having delays over the interval $[\tau - T_c/2, \tau + T_c/2]$. For uplink, the received signal at the base station can be written in a vector form as

$$\mathbf{x}(t) = \sum_{k=1}^{N} \sum_{l=1}^{L_k} \mathbf{h}_{u,k}^{(l)}(t) s_{u,k}\left(t - \tau_{u,k}^{(l)}\right) + \mathbf{n}(t) \tag{1}$$

where

L_k number of resolvable delay paths of user k;
$\mathbf{h}_{u,k}^{(l)}(t)$ and $\tau_{u,k}^{(l)}$ lth delay path channel response and time delay of user k, respectively;
$\mathbf{n}(t)$ receiver background noise vector, each element of which is an independent AWGN with one-sided spectrum density N_0.

For downlink, let $\mathbf{w}_{d,j}$ denote the downlink beamforming weight vector for user j, and assume mobile users have the same number of uplink and downlink delay paths. The received signal at mobile user k is given by

$$r_k(t) = \sum_{j=1}^{N} \sum_{l=1}^{L_k} \mathbf{w}_{d,j}^H \mathbf{h}_{d,k}^{(l)}(t) s_{d,j}\left(t - \tau_{d,k}^{(l)}\right) + u_k(t) \tag{2}$$

where $\mathbf{h}_{d,k}^{(l)}(t)$ and $\tau_{d,k}^{(l)}$ denote the downlink channel vector and time delay corresponding to the lth delay path of user k, respectively; and $u_k(t)$ is AWGN received at mobile k. We assume the one-sided spectrum density of $u_k(t)$ is $N_{d,k}$.

To establish uplink and downlink channel models mathematically, we use two parameters to describe each delay path: nominal DOA and angular spread. For example, for user k's lth delay path, if the nominal DOA is $\bar{\theta}_k^{(l)}$ and the angular spread is $\Delta_k^{(l)}$, then the DOA's of the multipath components for that delay path are uniformly distributed over $[\bar{\theta}_k^{(l)} - \Delta_k^{(l)}/2, \bar{\theta}_k^{(l)} + \Delta_k^{(l)}/2]$. We also use angular separation, Ξ_k, to describe the distribution of the nominal DOAs for all delay paths of user k. Specifically, the nominal DOAs, $\bar{\theta}_k^{(l)}$s, are assumed to be uniformly distributed over $[\Pi - \Xi_k/2, \Pi + \Xi_k/2]$, with Π uniformly distributed over the possible DOAs, say $[-\pi/3, \pi/3]$, if each cell is divided into three sectors.

Let us consider user k's lth delay path, and denote $\theta_{k,1}^{(l)} < \theta_{k,2}^{(l)} < \cdots < \theta_{k,p}^{(l)}$ as the DOAs for the multipath components of that delay path. The uplink steering vector, $\mathbf{a}_u(\theta)$ for signals arriving from DOA θ is: $\mathbf{a}_u(\theta) = [1, e^{j2\pi z \sin(\theta)/\lambda_u}, \ldots, e^{j2(m-1)\pi z \sin(\theta)/\lambda_u}]^T$, where z is antenna spacing, and λ_u is uplink wavelength. By denoting $\alpha_{u,i}(t)$ as the complex path strength of the signal coming from the ith DOA, it is seen that the uplink channel response is given by

$$\mathbf{h}_{u,k}^{(l)}(t) = \sum_{i=1}^{p} \alpha_{u,i}(t) \mathbf{a}_u\left(\theta_{k,i}^{(l)}\right) \tag{3}$$

Note $\alpha_{u,i}(t) = K_{u,k}\tilde{\alpha}_{u,i}(t)$, where $K_{u,k}$ is the combined uplink shadowing and path loss parameter for user k, and $\tilde{\alpha}_{u,i}(t)$ accounts for uplink fast fading effect. Here, we assume that the DOAs are time-invariant, which is reasonable since the change in direction of the mobile with respect to the base station is negligible during a small observation time, such as several time slots.

For FDD systems, according to reciprocal law, only the DOAs remain unchanged for uplink and downlink transmissions [16]. Thus, the downlink channel response can be written as

$$\mathbf{h}_{d,k}^{(l)}(t) = \sum_{i=1}^{p} \alpha_{d,i}(t) \mathbf{a}_d\left(\theta_{k,i}^{(l)}\right) \tag{4}$$

where

$$\mathbf{a}_d(\theta_{k,i}^{(l)}) = [1, e^{j2\pi z \sin(\theta_{k,i}^{(l)})/\lambda_d}, \ldots, e^{j2(m-1)\pi z \sin(\theta_{k,i}^{(l)})/\lambda_d}]^T$$

is the downlink steering vector at DOA $\theta_{k,i}^{(l)}$. Here λ_d is the downlink wavelength, $\alpha_{d,i}(t) = K_{d,k}\tilde{\alpha}_{d,i}(t)$ is the complex path strength of the signal leaving for the kth DOA with $K_{d,k}$ being the combined downlink shadowing and path loss parameter for user k, and $\tilde{\alpha}_{d,i}(t)$ accounts for downlink fast fading effect.

III. Uplink Beamforming and Power Control

A. Single-Cell Environment

Denote γ_u as the required SIR value, $\mathbf{p}_u^{(s)}$ the power vector which consists of the received powers normalized by the background noise power density. The optimal uplink weight and power vectors can be determined via joint uplink beamforming and power control technique (UBPCT) [2], [10]. For PUPW beamforming scheme, given the converged beamforming weights, $\mathbf{w}_{u,1}, \ldots, \mathbf{w}_{u,N}$, the power vector can be determined by [10]

$$\left(\mathbf{I} - \gamma_u \mathbf{F}_u^{(s)}\right) \mathbf{p}_u^{(s)} = \gamma_u \mathbf{g}_u^{(s)} \tag{5}$$

which yields

$$\mathbf{p}_u^{(s)} = \gamma_u \left(\mathbf{I} - \gamma_u \mathbf{F}_u^{(s)}\right)^{-1} \mathbf{g}_u^{(s)} \tag{6}$$

where

$$\mathbf{p}_u^{(s)} = [P_{u,1}^{(s)} T/N_0, \ldots, P_{u,N}^{(s)} T/N_0]^T$$

$$\mathbf{g}_u^{(s)} = \left[(\|\mathbf{w}_{u,1}\|^2)/(\sum_{l=1}^{L_1} |\mathbf{w}_{u,1}^H \mathbf{h}_{u,1}^{(l)}|^2), \ldots \right.$$
$$\left. (\|\mathbf{w}_{u,N}\|^2)/(\sum_{l=1}^{L_N} |\mathbf{w}_{u,N}^H \mathbf{h}_{u,N}^{(l)}|^2)\right]^T$$

and

$$\left[\mathbf{F}_u^{(s)}\right]_{i,j} = \begin{cases} \dfrac{r_u(i)}{G}\left(1 - \dfrac{\sum_{l=1}^{L_i} \left|\mathbf{w}_{u,i}^H \mathbf{h}_{u,i}^{(l)}\right|^4}{\left(\sum_{l=1}^{L_i} \left|\mathbf{w}_{u,i}^H \mathbf{h}_{u,i}^{(l)}\right|^2\right)^2}\right), & \text{if } i = j \\ \dfrac{r_u(j)}{G} \dfrac{\sum_{l=1}^{L_j} \left|\mathbf{w}_{u,i}^H \mathbf{h}_{u,j}^{(l)}\right|^2}{\sum_{l=1}^{L_i} \left|\mathbf{w}_{u,i}^H \mathbf{h}_{u,i}^{(l)}\right|^2}, & \text{if } i \neq j \end{cases} \tag{7}$$

The average total received power at the base station is given by

$$P_T^{(s)} = E\left[\mathbf{1}^T \mathbf{R}_u \mathbf{p}_u^{(s)}\right] = \gamma_u \bar{\mu}_u^{(s)} \tag{8}$$

where $\bar{\mu}_u^{(s)} = E[\mathbf{1}^T \mathbf{R}_u (\mathbf{I} - \gamma_u \mathbf{F}_u^{(s)})^{-1} \mathbf{g}_u^{(s)}]$ with $\mathbf{R}_u = \mathrm{diag}[r_u(1), \ldots, r_u(N)]$, and $E[\cdot]$ represents statistical expectation over DOA.

For uplink, power constraint is specified for each mobile user. The system capacity can be evaluated by determining the maximum number of users with which the outage probability is less than certain value, say 0.01, given a certain power constraint. By outage probability, we mean the probability with which the maximum achievable SIR value is less than the prescribed SIR value.

B. Multiple-Cell Environment

In this subsection, we extend the single-cell results into multiple-cell environment. The main idea involved with the analysis is that while the received powers at the base station from the users within the own cell is specific in the sense that they are dependent on the given spatial distribution of users within the same cell, the overall interference power from intercells is almost constant as it is a statistical value. We model the intercell interference as an AWGN process whose power (normalized by background noise power density) is proportional to the average intracell interference power, denoted as $P_{T,u}^{(m)}$. Here, $P_{T,u}^{(m)}$ is also normalized by the background noise power density. The proportional coefficient, c_u, is dependent on the distance-dependent path loss decay law index, α, standard deviation of the shadowing effect, σ, as well as multipath fading and power control error. When multipath fading and power control error are neglected, $c_u = 0.57$ for $\alpha = 4$ and $\sigma = 8$ [9]. In Appendix A, it is shown that the intracell interference power is given by

$$P_{T,u}^{(m)} = \frac{G P_{T,u}^{(s)}}{G - c_u P_{T,u}^{(s)}} \tag{9}$$

In order to keep $P_{T,u}^{(m)}$ as a positive value, $P_{T,u}^{(s)}$ should satisfy the following condition

$$P_{T,u}^{(s)} < \frac{G}{c_u} = P_{u,\infty} \tag{10}$$

which means that the single-cell average total received power should be less than a predetermined constant, $P_{u,\infty}$, in order for the multiple-cell systems to support the same number of users for each sector. When $G = 16, P_{u,\infty} = 14.26$ dB for $c_u = 0.6$, and $P_{u,\infty} = 16.02$ dB for $c_u = 0.4$.

When both single- and multiple-cell have the same number of users, $P_{T,u}^{(m)} > P_{T,u}^{(s)}$. Usually, $P_{T,u}^{(m)}$ has a maximum value, $P_{u,0}$, say 30 dB. From (9), a more strict condition should be satisfied

$$P_{T,u}^{(s)} < \frac{G P_{u,0}}{G + c_u P_{u,0}} = P_{u,c}. \tag{11}$$

Therefore, for multiple-cell case, the system capacity is determined by the maximum number of users with which the corresponding single cell average total received power is less than $P_{u,c}$.

IV. Downlink Beamforming and Power Control

A. Single-Cell Environment

In downlink, beamforming is implemented at the base station, and the beamforming weights should be predetermined. In [11], iterative virtual power weighted (IVPW) or virtual power weighted (VPW) algorithms were proposed to realize virtual UBPCT. In the next section, we will also propose two suboptimal algorithms to generate downlink beamforming weights.

Denote $\mathbf{p}_d^{(s)}$ as the downlink power vector consisting of the transmitted powers normalized by the background noise power density as seen at the cell boundary, and γ_d the required SIR value. Once downlink beamforming weights are determined, fast transmit power technique [5] can be used to adjust the transmit powers while maintaining the SIR requirements. Mathematically, the downlink power vector can also be determined by [11]

$$\left(\mathbf{I} - \gamma_d \mathbf{F}_d^{(s)}\right) \mathbf{p}_d^{(s)} = \gamma_d \mathbf{g}_d^{(s)} \tag{12}$$

where

$$\mathbf{p}_d^{(s)} = [R^{-\alpha} P_{d,1}^{(s)} T/N_0, \ldots, R^{-\alpha} P_{d,N}^{(s)} T/N_0]^T$$

$$\mathbf{g}_d^{(s)} = \left[((d_1/R)^\alpha)/(\sum_{l=1}^{L_1} |\mathbf{w}_{d,1}^H \mathbf{h}_{d,1}^{(l)}|^2), \ldots \right.$$
$$\left. ((d_N/R)^\alpha)/(\sum_{l=1}^{L_N} |\mathbf{w}_{d,N}^H \mathbf{h}_{d,N}^{(l)}|^2)\right]^T$$

and, see (13) at the bottom of the page, with d_k being the distance between the base station and the kth user; R the cell radius. Here we have assumed that the AWGN noise powers are equal for every mobile users and ignored the shadowing effect. From (12), $\mathbf{p}_d^{(s)}$ is DOA and distance dependent. The average total transmitted power seen at the cell boundary is given by

$$P_{T,d}^{(s)} = E\left[\mathbf{1}^T \mathbf{R}_d \mathbf{p}_d^{(s)}\right] = \gamma_d \bar{\mu}_d^{(s)} E_r \tag{14}$$

$$\left[\mathbf{F}_d^{(s)}\right]_{i,j} = \begin{cases} \dfrac{r_d(i)}{G}\left(1 - \dfrac{\sum_{l=1}^{L_i} \left|\mathbf{w}_{d,i}^H \mathbf{h}_{d,i}^{(l)}\right|^4}{\left(\sum_{l=1}^{L_i} \left|\mathbf{w}_{d,i}^H \mathbf{h}_{d,i}^{(l)}\right|^2\right)^2}\right), & \text{if } i = j \\ \dfrac{r_d(j)}{G}\left(\dfrac{\sum_{l=1}^{L_i} \left|\mathbf{w}_{d,j}^H \mathbf{h}_{d,i}^{(l)}\right|^2}{\sum_{l=1}^{L_i} \left|\mathbf{w}_{d,i}^H \mathbf{h}_{d,i}^{(l)}\right|^2} - \dfrac{\sum_{l=1}^{L_i} \left|\mathbf{w}_{d,i}^H \mathbf{h}_{d,i}^{(l)}\right|^2 \left|\mathbf{w}_{d,j}^H \mathbf{h}_{d,i}^{(l)}\right|^2}{\left(\sum_{l=1}^{L_i} \left|\mathbf{w}_{d,i}^H \mathbf{h}_{d,i}^{(l)}\right|^2\right)^2}\right), & \text{if } i \neq j \end{cases} \tag{13}$$

where $E_r = E[(r/R)^\alpha] = 2/(\alpha+2)$ (Note: $p(r) = 2r/R^2$), $\bar{\mu}_d^{(s)} = E[\mathbf{1}^T\mathbf{R}_d(\mathbf{I} - \gamma_d\mathbf{F}_d^{(s)})^{-1}\tilde{\mathbf{g}}_d^{(s)}]$ with $\mathbf{R}_d = \text{diag}[r_d(1), \ldots, r_d(N)]$ and $\tilde{\mathbf{g}}_d^{(s)} = [1/(\sum_{l=1}^{L_1}|\mathbf{w}_{d,1}^H\mathbf{h}_{d,1}^{(l)}|^2), \ldots, 1/(\sum_{l=1}^{L_N}|\mathbf{w}_{d,N}^H\mathbf{h}_{d,N}^{(l)}|^2)]^T$.

For downlink, power constraint is specified for total transmitted power (normalized by the background noise spectrum density) provided by the base station. The system capacity can be evaluated by determining the maximum number of users with which the outage probability is equal to a certain value, say 0.01, given a certain power constraint value. For single-cell case, we may try to maximize the maximum achievable SINR values such that the systems can support more and more users. Methods for doing this need not consider too much about the power constraint as the background noise power can be neglected.

B. Multiple-Cell Environment

1) Outer Cell Interference: For multiple-cell systems, although each outer cell may have different total transmitted power due to randomness of the DOAs and path distances of its own users, the total intercell interference seen at the specific cell may be considered as an AWGN process whose variance is proportional to the average intracell interference power, denoted as $P_{T,d}^{(m)}$. Different from uplink case, each mobile user right here receives intercell interference with different powers [8], $v_k P_{T,d}^{(m)}$, where $v_k = R_{0,k}^\alpha \sum_{i=1}^{N_c-1} R_{i,k}^{-\alpha}$ with $R_{0,k}$ being the distance between the specific mobile user and its own base station, $R_{i,k}$s the distances between the specific user to other outer cell base stations.

In Appendix B, it is shown that the average intracell interference power is given by

$$P_{T,d}^{(m)} = \frac{GE_r P_{T,d}^{(s)}}{GE_r - c_d P_{T,d}^{(s)}} \tag{15}$$

where $c_d = E[v_k]$. In order to keep $P_{T,d}^{(m)}$ as a positive value, $P_{T,d}^{(s)}$ should satisfy the following condition

$$P_{T,d}^{(s)} < \frac{GE_r}{c_d} = P_{d,\infty} \tag{16}$$

More strictly, for downlink transmission, the total transmitted power seen at the cell boundary has a limit, $P_{d,0}$, i.e., $P_{T,d}^{(m)} \le P_{d,0}$. Therefore, in order for multicell cases to satisfy the same power constraint, the maximum single cell average total transmitted power should satisfy

$$P_{T,d}^{(s)} < \frac{GE_r P_{d,0}}{GE_r + c_d P_{d,0}} = P_{d,c} \tag{17}$$

Table I shows $P_{d,c}$ values with respect to different $P_{d,0}$s and c_ds for $G = 16$ and $G = 128$.

2) Downlink Multiple-Cell Capacity Determination Method: If power constraint is not added, single- and multiple-cell cases may yield same outage probability when same number of users is considered. This is not the case when power constraint is considered. Specifically, for single–cell case, since the noise power is relatively small, the outage probability without power constraint will approach that with relatively larger power constraint, say 20 dB. However, for multiple-cell case, since the noise power is relatively larger than that in single–cell case, to achieve same outage probability, the required power constraint for multiple-cell case will be much larger than that for single–cell case. Therefore, power constraint should be considered in determining multiple-cell capacity of DS-CDMA systems.

TABLE I
$P_{d,c}$ VALUES (IN dB) WITH RESPECT TO DIFFERENT $P_{d,0}$S AND c_dS: $\alpha = 4.0$

(c_d, G)	$P_{d,0}$ = 10dB	$P_{d,0}$ = 20dB	$P_{d,0}$ = 30dB	$P_{d,0}$ = 40dB	$P_{d,0} = \infty$
(0.6, 16)	6.7264	9.1186	9.4500	9.4846	9.4885
(0.5, 16)	7.1276	9.8401	10.2342	10.2757	10.2803
(0.4, 16)	7.5696	10.7058	11.1919	11.2436	11.2494
(0.3, 16)	8.0618	11.7881	12.4222	12.4911	12.4988
(0.2, 16)	8.6170	13.2331	14.1454	14.2481	14.2597
(0.6, 128)	9.4286	16.1866	18.2210	18.4886	18.5194
(0.5, 128)	9.5187	16.6317	18.9556	19.2743	19.3112
(0.4, 128)	9.6108	17.1276	19.8401	20.2342	20.2803
(0.3, 128)	9.7049	17.6875	20.9522	21.4683	21.5297
(0.2, 128)	9.8011	18.3305	22.4508	23.1989	23.2906

The algorithm for determining downlink multicell capacity consists of the following steps.

(1.1) Calculate single cell average total transmitted powers, $P_{T,d}^{(s)}$s, using Monte Carlo simulations for different number of users;
(1.2) Compute multiple-cell average total transmitted powers, $P_{T,d}^{(m)}$s via (15).
(1.3) Perform Monte Carlo simulations to obtain statistics of total transmitted powers, $P_d^{(m)}$s, using (23) in Appendix B, for different DOAs and distances.
(1.4) Calculate outage probability $P_{\text{out}} = \Pr\{P_d^{(m)} > P_{d,0}\}$ for given power constraints, $P_{d,0}$s.
(1.5) Determine system capacity with respect to different power constraints.

There are two ways to simplify the simulation complexity. First, in step (1.1), for given number of users, $P_{T,d}^{(s)}$ is the average total transmitted power over the random variables, DOA and distance. Denote $\bar{P}_{T,d}^{(s)}$ as the average total transmitted power over the random variable DOA when all users are along the cell boundary. From (14), we have $P_{T,d}^{(s)} = E_r\bar{P}_{T,d}^{(s)}$. Therefore, only $\bar{P}_{T,d}^{(s)}$ needs to be evaluated. Second, in step (1.3), as the downlink beamforming weights are independent of the path losses [15], we may first vary the DOAs and set $d_k = R$ for all ks, and compute $\mathbf{F}_d^{(s)}$ in (23) in Appendix B, then vary the distances to generate $\mathbf{g}_d^{(m)}$ in (23), thus obtain the $\mathbf{p}_d^{(m)}$ for that specific set of DOAs and distances. Therefore, for a given set of DOAs, many (say 1000) total transmitted powers are obtained, which are dependent on different combination of distances; however, only one $\mathbf{F}_d^{(s)}$ in (23) needs to be computed.

V. Downlink Beamforming by Modifying Uplink Weights

In [11], V-UBPCT algorithm is developed to generate downlink beamforming weights. Even though V-UBPCT yields optimal solution to downlink beamforming problem, same as other traditional downlink beamforming schemes, it is difficult for implementation in practice as it requires downlink channel responses and complicated computations. In this section, we first review algorithm steps of UBPCT for uplink and V-UBPCT for downlink; then compare the generated beam patterns of optimal uplink and downlink weights; finally, two new downlink beamforming algorithms are proposed by modifying uplink weights for FDD DS-CDMA.

A. Algorithm Steps of Real and Virtual UBPCTs

First, let us examine how the optimal uplink and downlink beamforming weights are obtained. To minimize all mobiles' transmitted powers individually, uplink uses real UBPCT method to generate uplink beamforming weights [10]; downlink, however, employs virtual UBPCT method to generate downlink beamforming weights in order to minimize the total transmitted power [11], [15]. Real and virtual UBPCTs involve the following similar iterative steps.

(2.1) Choose an initial real (virtual) uplink power vector;
(2.2) Compute the real (virtual) uplink weight vectors for given real (virtual) uplink power vector;
(2.3) Adjust the real (virtual) uplink power vector for given real (virtual) uplink weight vectors;
(2.4) Update (2.2) and (2.3) until the power and weight vectors are converged.

In real UBPCT, the real uplink channel responses are involved in the adaptive process. In virtual UBPCT, however, the downlink channel responses are set to be the virtual uplink channel responses, and the generated virtual uplink beamforming weights are used as the real downlink beamforming weights. In steps (2.2) and (2.3), orthogonality of downlink codes has been considered for virtual UBPCT. However, when the number of multipaths becomes large, or the orthogonality of downlink codes is ignored, the real UBPCT is actually the counterpart of the virtual UBPCT.

B. Beam Pattern Comparison

Let us compare the uplink and downlink beam patterns generated by the real and virtual UBPCTs. Denote $\mathbf{w}_{u,k} = [w_{u,k}(1), \ldots, w_{u,k}(M)]^T$ and $\mathbf{w}_{d,k} = [w_{d,k}(1), \ldots, w_{d,k}(M)]^T$ as, respectively, the converged uplink and downlink beamforming weight vectors for the kth user. Although the generated uplink beam response, $P_{u,k}(\theta) = |\mathbf{w}_{u,k}\mathbf{a}_u(\theta)|^2$, is not always equal to the generated downlink one, $P_{d,k}(\theta) = |\mathbf{w}_{d,k}\mathbf{a}_d(\theta)|^2$, at every DOA, these two responses do have some similarities, especially for the main beam and null positions, which are of vital importance for both links. As we are more concerned about how to increase the system capacity or how to support more high rate users using adaptive antenna array, we consider the cases in which the system is working in the near full capacity, or the system has some very high rate users. In those cases, on one hand, both uplink and downlink direct their main beams toward the desired user. On the other hand, uplink employs nulls to null out stronger interfering users, such as high rate users; while for downlink, nulls are directed to high rate users such that these users will receive less interference pollution. In particular, the criteria of putting nulls by this way are that, for uplink, all users' transmitted powers are minimized individually; while for downlink, the total transmitted power is minimized in order for all users to work in the prescribed SINR values. Therefore, for symmetric traffic environment, both links' patterns put common nulls at the high rate users, while maintain the same main beams.

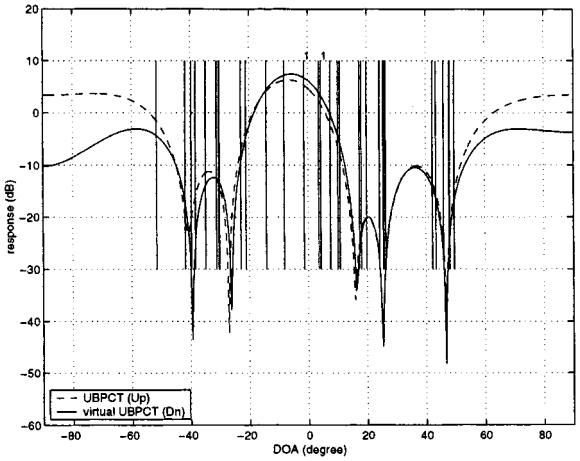

Fig. 2. Generated uplink and downlink beam patterns using real and virtual UBPCTs.

Fig. 2 shows the generated uplink and downlink beam patterns using real and virtual UBPCTs, respectively. Here, user 1 is the interesting user, the other 19 users are interfering users, and $f_u = 1.8$ GHz, $f_d = 2.0$ GHz, and the processing gain is 16. These beam patterns are obtained by increasing the target SIR to certain value, which is also equivalent to increase the total user number. It is seen that both links have very near positions for both main beams and nulls.

C. Downlink Beamforming by Modifying Uplink Weights for FDD

In view of the similarities between the generated beam patterns using real and virtual UBPCTs, downlink beamforming weights can be generated by modifying uplink beamforming weights. Two suboptimal algorithms are proposed to constrain the same positions for nulls and main beams: NC algorithm, which maintains the same null positions for both uplink and downlink beam patterns, and FC algorithm, which constrains same main beam position for both beam patterns. Since uplink beamforming weights are ready information at the base station [3], the new algorithms are easy for implementation.

1) NC Algorithm: The NC algorithm consists of the following steps.

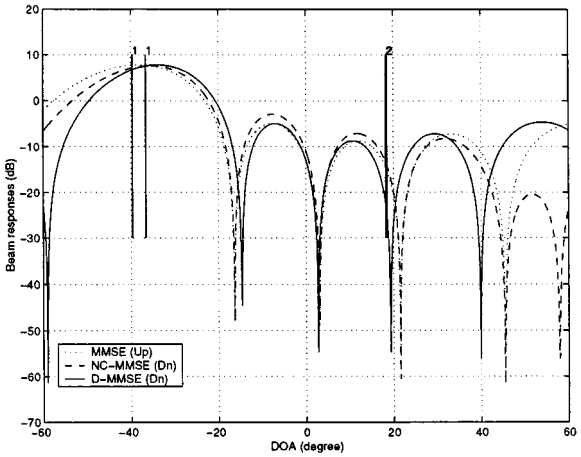

Fig. 3. Generated beam patterns using NC method.

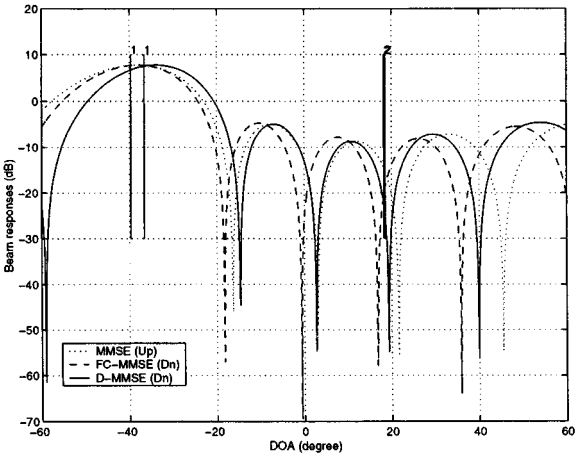

Fig. 4. Generated beam patterns using FC method.

(3.1) Determine the uplink beam pattern's nulls, $z_{u,k}(i), i = 1,\ldots,M-1$, using the polynomial formed from the uplink weights:

$$\sum_{i=1}^{M} w_{u,k}(i)z^{-i+1} = w_{u,k}(1)(1-z_{u,k}(1)z^{-1})\ldots(1-z_{u,k}(M-1)z^{-1}) \tag{18}$$

(3.2) Transform the phase components of the uplink beam pattern's nulls, and obtain the phase components of downlink beam pattern's nulls as $\phi_{d,i} = (f_d/f_u)\phi_{u,i}$, where $z_{u,k}(i) = A_{u,k}(i)e^{j\phi_{u,k}(i)}$, for $i = 1,\ldots,M-1$.

(3.3) Construct the downlink beam pattern's nulls as $z_{d,k}(i) = A_{d,k}(i)e^{j\phi_{d,k}(i)}$ with $A_{d,k}(i) = A_{u,k}(i)$ or simply $A_{d,k}(i) = 1$ for $i = 1,\ldots,M-1$.

(3.4) Construct the downlink beamforming weight vector:

$$\sum_{i=1}^{M} w_{d,k}(i)z^{-i+1} = w_{d,k}(1)(1-z_{d,k}(1)z^{-1})\ldots(1-z_{d,k}(M-1)z^{-1}) \tag{19}$$

Fig. 3 shows an example of generated uplink beam pattern by UBPCT, denoted as MMSE (up), and generated downlink beam patterns using NC-MMSE and D-MMSE methods. Here, NC-MMSE modifies uplink weights for downlink using NC method; while D-MMSE uses uplink weights for downlink directly. The NC algorithm keeps same null positions for both uplink and downlink beam patterns. It is expected that NC algorithm is powerful for capacity enhancement for single cell, symmetric traffic environments. However, for asymmetric traffic environment, the NC algorithm may be far away from the optimal solution.

2) FC Algorithm: In [12], frequency calibrated algorithm was proposed to estimate downlink channel covariance matrix (DCCM) for FDD systems using uplink channel covariance matrix (UCCM). In this paper, we apply this algorithm to estimate downlink beamforming weights using uplink ones. FC algorithm involves the following steps.

(4.1) Construct uplink weight covariance matrix (UWCM): $\mathbf{Q}_{u,k} = (1/P)\sum_{i=1}^{P}\mathbf{w}_{u,k}(i)\mathbf{w}_{u,k}^{H}(i)$, where P is the number of samples;

(4.2) Estimate downlink weight covariance matrix (DWCM), $\mathbf{Q}_{d,k}$;

(4.3) Compute the principal eigenvector of DWCM, and set it as the downlink beamforming weight vector.

In step (4.2), for uniform linear array, a fast computation method exists for estimating DWCM if the UWCM and DWCM are made to be Toeplitz. Denote $\mathbf{q}_{u,k}^{(r)}$ and $\mathbf{q}_{d,k}^{(r)}$ as the real part of the first column of $\mathbf{Q}_{u,k}$ and $\mathbf{Q}_{d,k}$, respectively; $\mathbf{q}_{u,k}^{(i)}$ and $\mathbf{q}_{d,k}^{(i)}$ as the imaginary part of the first column (excluding the first element) of $\mathbf{Q}_{u,k}$ and $\mathbf{Q}_{d,k}$, respectively. Then, we have

$$\mathbf{q}_{d,k}^{(r)} = \mathbf{B}_r\mathbf{q}_{u,k}^{(r)} \quad \text{and} \quad \mathbf{q}_{d,k}^{(i)} = \mathbf{B}_i\mathbf{q}_{u,k}^{(i)} \tag{20}$$

Here, $\mathbf{B}_r$ and $\mathbf{B}_i$ are called FC matrices, which are dependent on uplink and downlink carrier frequencies, geometry of base station antenna array and cell sectorization. Please refer to [12] for some examples of FC matrices. Fig. 4 shows an example of generated downlink beam patterns using FC method and D-MMSE method. It is pointed out that the generated downlink weight vector via FC algorithm is equivalent to the downlink steering vector whose DOA is equal to the maximum point of the uplink beam pattern. Therefore, FC algorithm is also called peak constrained (PC) method.

VI. Performance Evaluation Through Computer Simulations

Computer simulations were carried out to evaluate the capacity of DS-CDMA systems with antenna array via PUPW beamformer. A six-element ULA is equipped for each sector (three sectors per cell). Macrocell systems are considered in which the angular separation between each delay path of the same user is within 10°, and the angular spread for each delay path is 1°. Each user is with two delay paths and the processing gain is $G = 16$. The required SIR threshold is chosen to be $\gamma_{u,0} = \gamma_{d,0} = 6.8$ dB. We also choose $f_u = 1.8$ GHz, $f_d = 2.0$ GHz and $z = \lambda_u/2$.

The following downlink beamforming algorithms are compared.

TABLE II
$P_{T,u}^{(s)}$ AND $P_{T,u}^{(m)}$ VALUES (IN dB) FOR DIFFERENT DATA RATE DISTRIBUTION: $G = 16$, $c_u = 0.6$

User No.	8	9	10	11	12	13	14	15
$P_{T,u}^{(s)}$, Type 1	6.5766	7.2603	7.8752	8.5247	9.1179	9.6663	10.1254	10.8765
$P_{T,u}^{(s)}$, Type 2	6.6513	7.3878	7.9998	8.6802	9.2438	9.8415	10.3917	11.0146
$P_{T,u}^{(m)}$, Type 1	7.3883	8.2270	9.0097	9.8736	10.7047	11.5189	12.2436	13.5417
$P_{T,u}^{(m)}$, Type 2	7.4786	8.3869	9.1723	10.0871	10.8874	11.7904	12.6860	13.8021

- D-MMSE/D-MRC: Uplink MMSE/MRC weights are used for downlink directly.
- FC-MMSE, NC-MMSE/FC-MRC, NC-MRC: Uplink MMSE/MRC weights are first processed via FC/NC algorithms, then used for downlink.
- IVPW-1/VPW-1: IVPW/VPW algorithms [11] are used to estimate downlink beamforming weights with estimated downlink equivalent one-path channel vectors (EOCVs) as input.
- IVPW-T: Algorithm A in [15] is used to estimate downlink beamforming weights with true downlink multidelay channel vectors as input.
- IVPW-A: Uplink multidelay path vectors are used to determine downlink multidelay path channel vectors via FC algorithm, then Algorithm A in [15] is employed to estimate downlink beamforming weights with the estimated downlink multidelay channel vectors as input.

Real UBPCT in [10] is used to generate uplink MMSE weights; while uplink MRC weight vector is equal to the principal eigenvector of the UCCM. Two types of data rate distributions are evaluated.

- *Type 1 (Symmetric Traffic):* Uplink data rates are chosen to be $r_u(k) = 0.5$, for $k = 1, \ldots, N$; downlink data rates are $r_d(k) = 1.0$, for $k = 1, \ldots, N$;
- *Type 2 (Asymmetric Traffic):* Uplink data rates are randomly chosen from $\{0.1, 0.2, \ldots, 1.0\}$ with total data rate $\sum_{i=1}^{N} r_u(i) = 0.5N$, while downlink data rates are from $\{0.2, 0.4, \ldots, 2.0\}$ with $\sum_{i=1}^{N} r_d(i) = N$.

Table II shows the single-cell average uplink total transmitted powers, $P_{T,u}^{(s)}$, with respect to different number of users. Using (15), the multicell average uplink total transmitted powers, $P_{T,u}^{(m)}$, with respect to different number of users are also given in Table II. These values will be used in (21) in Appendix A when the uplink beamforming weights are to be determined for multicell environment.

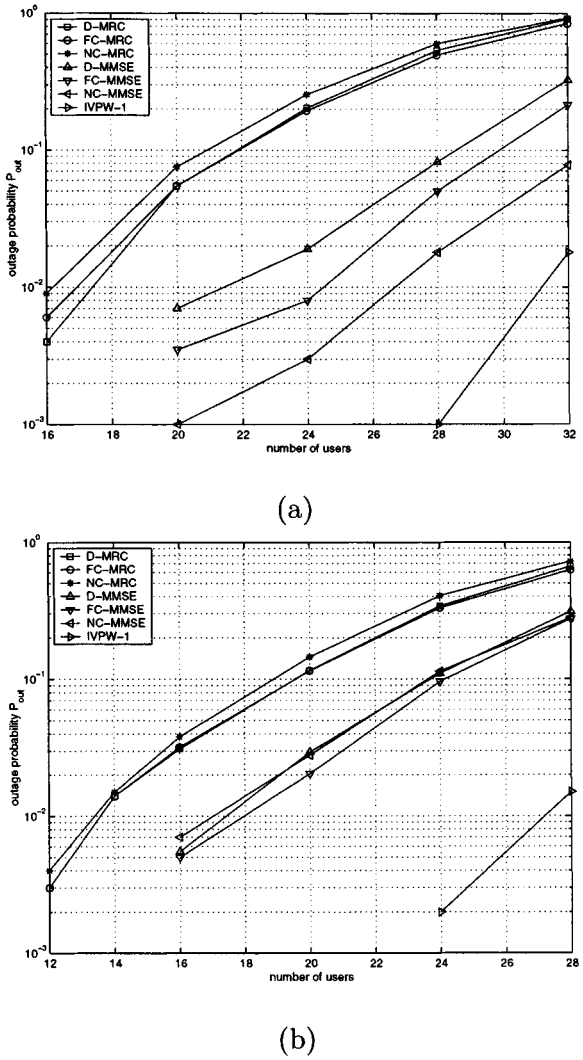

Fig. 5. Single cell outage probability for different algorithms with respect to number of users. (a) Type 1 traffic. (b) Type 2 traffic.

A. Single Cell Capacity

Fig. 5(a) shows the outage probability with respect to different number of users for Type 1 data rate distribution. It is seen that IVPW-1 is the best among the algorithms compared, which can support 31 users. NC-MMSE, FC-MMSE and D-MMSE can support 26, 24, and 21 users, respectively, showing that NC-MMSE is the best among the suboptimal algorithms based on uplink MMSE weights for symmetric traffic. For uplink MRC weight-based algorithms, D-MRC, NC-MRC and FC-MRC can support 17, 16, and 16 users, respectively. Fig. 5(b) illustrates the results obtained for Type 2 data rate distribution. It is obvious that IVPW-1 can support 27 users, and the uplink MMSE weight-based algorithms are still better than uplink MRC weight-based algorithms. However, for asymmetric traffic, the NC-MMSE is a little bit worse than FC-MMSE.

TABLE III
$P_{T,d}^{(s)}$ VALUES (IN dB) FOR DIFFERENT ALGORITHMS: $G = 16$, TYPE 1

User No.	8	9	10	11	12	13	14	15
D-MMSE	5.7082	6.4577	7.1165	7.7596	8.3978	9.0253	9.7216	10.2389
FC-MMSE	5.2869	5.9860	6.5985	7.2803	7.8922	8.4821	9.1599	9.6233
NC-MMSE	5.6172	6.3596	7.0222	7.6667	8.2743	8.8958	9.5267	10.0525
D-MRC	5.8256	6.6073	7.3160	8.0646	8.8289	9.4110	10.1086	10.8426
FC-MRC	5.3281	6.0842	6.7924	7.5433	8.1520	8.8096	9.5578	10.1412
NC-MRC	5.7275	6.5043	7.4153	7.9357	8.6187	9.3639	10.7139	10.8333
IVPW-1	5.2635	5.9553	6.5723	7.2411	7.8456	8.4129	9.0373	9.5427
VPW-1	5.2638	5.9558	6.5733	7.2792	7.8509	8.4236	9.0058	9.5779
IVPW-A	5.2671	5.9549	6.5725	7.2415	7.8760	8.4087	9.0412	9.5350
IVPW-T	5.2345	5.9251	6.5409	7.2060	7.8041	8.3684	8.9654	9.4857

TABLE IV
$P_{T,d}^{(s)}$ VALUES (IN dB) FOR DIFFERENT ALGORITHMS: $G = 16$, TYPE 2

User No.	8	9	10	11	12	13	14	15
D-MMSE	6.0465	6.7927	8.3154	8.3619	8.9682	9.6390	10.4360	11.1078
FC-MMSE	5.5984	6.3761	7.0476	7.7321	8.4519	9.2730	9.8397	10.5742
NC-MMSE	5.9684	6.7080	7.4487	8.2695	8.8611	9.8708	10.1965	11.0782
D-MRC	6.1752	6.9413	7.7754	8.7868	9.4693	10.1757	10.9752	11.8143
FC-MRC	5.6894	6.4330	7.2533	8.2011	8.9074	9.9223	10.4309	11.1661
NC-MRC	6.0957	6.8642	7.7620	8.6762	9.4596	10.1486	10.8150	11.8134
IVPW-1	5.5305	6.2809	6.9243	7.6208	8.2300	8.8309	9.3697	10.0884
VPW-1	5.5409	6.2874	6.9399	7.6188	8.2953	8.8690	9.4301	10.2303
IVPW-A	5.5299	6.2944	6.9979	7.5888	8.2154	8.8122	9.3558	10.0696
IVPW-T	5.4994	6.2469	6.8846	7.5522	8.1648	8.7633	9.2996	9.9875

B. Multicell Capacity

Tables III and IV show the single cell average downlink total transmitted powers, $P_{T,d}^{(s)}$s, with respect to different number of users for Type 1 and Type 2 data rate distribution using different downlink beamforming algorithms, respectively. Tables V and VI compare the required multicell average downlink total transmitted powers, $P_{T,d}^{(m)}$, for Type 1 and Type 2 data rate distributions, respectively. From Tables V and VI, it is seen that using different downlink beamforming approaches, the required average downlink total transmitted powers are quite different; and at the extreme, when the number of users is large enough, the required total transmitted power may become negative, which implies that the system cannot support that number of users when that particular algorithm is used. Therefore, from these tables, a rough estimate of the system capacity can be obtained.

Further analysis is conducted for downlink multicell capacity when power constraint is considered. Fig. 6 compares the outage probability with respect to different power constraint using different algorithms for several user numbers. The multicell capacity results based on this figure as well as those for other user numbers (not given out here due to space limitations) are shown in Table VII.

From the simulation results, we have the following observations.

- Centralized algorithms, IVPW-1, VPW-1, IVPW-A, and IVPW-T, are better than the other decentralized algorithms. Specifically, IVPW-T is the optimal solution in terms of system capacity enhancement and power consumption. Uplink MRC-based algorithms, D-MRC and FC-MRC and NC-MRC, provide smallest system capacity among the methods compared. This is because that these algorithms just keep the main beam of downlink beam pattern toward the intended user (D-MRC also has certain DOA shift), but do not consider the interference polluted to the other users.
- Although different algorithms may have same system capacity, the required average total transmitted powers may be quite different. Specifically, for D-MRC and FC-MRC, although both of them can support 13 users for Type 1 distribution, the required total transmitted power for D-MRC is about 9.7 dB higher than that required by FC-MRC.
- FC-MMSE is the best decentralized algorithm. More specifically, for both Type 1 and Type 2 data rate distributions, FC-MMSE can support one more user than the other decentralized algorithms; and for same number of users, FC-MMSE costs less power. For example, for Type 2 and $N = 12$, the required power for FC-MMSE is about 2.4 dB less than that for NC-MMSE, and about 18 dB less than that for D-MRC.

VII. CONCLUSION

In this paper, we have proposed two suboptimal algorithms for generating downlink beamforming weights for FDD DS-CDMA mobile radio. These algorithms are very simple in implementation and computation as they just require the uplink weights as input. Multicell capacity are also analyzed using joint beamforming and power control scheme. Simulations have shown that for single cell cases, NC-MMSE is better than FC-MMSE for symmetric traffic, and similar to FC-MMSE for asymmetric traffic; while for multicell cases, FC-MMSE is better than NC-MMSE, and near the optimal solution in terms of power consumption and multicell capacity. When uplink uses MRC-based beamforming scheme, FC-MRC is much better than D-MRC and NC-MRC in terms of power consumption. Finally, it is pointed out that NC/FC algorithms can also be applied to downlink weight generation for TDMA/FDMA based FDD SDMA systems.

APPENDIX

A. Intracell Interference for Uplink Multiple-Cell Environment

For multiple-cell environment, we may still use joint beamforming and power control scheme to determine the beamforming weights and power vector. When the solution is converged, the power vector can be computed by, if same number of users is considered for both single- and multiple-cell cases,

$$\left(\mathbf{I} - \gamma_u \mathbf{F}_u^{(s)}\right) \mathbf{p}_u^{(m)} = \gamma_u \mathbf{g}_u^{(m)} \tag{21}$$

TABLE V
REQUIRED $P_{T,d}^{(m)}$ VALUES (IN dB) FOR DIFFERENT ALGORITHMS: $G = 16$, $c_d = 0.6$, TYPE 1

User No.	8	9	10	11	12	13	14	15
D-MMSE	8.0648	9.4477	10.8754	12.5956	14.9326	18.9752	-	-
FC-MMSE	7.3633	8.5543	9.7326	11.2752	13.0126	15.3258	20.5347	-
NC-MMSE	7.9093	9.2545	10.6546	12.3187	14.4023	17.8384	-	-
D-MRC	8.2687	9.7507	11.3653	13.6002	17.3397	26.9359	-	-
FC-MRC	7.4300	8.7333	10.1414	11.9679	13.9213	17.2046	-	-
NC-MRC	8.0979	9.5409	11.6222	13.1557	16.0301	24.8496	-	-
IVPW-1	7.3257	8.4990	9.6787	11.1776	12.8629	15.0010	19.0953	-
VPW-1	7.3261	8.4998	9.6809	11.2725	12.8799	15.0500	19.1350	-
IVPW-A	7.3315	8.4982	9.6792	11.1786	12.9602	14.9819	18.9351	-
IVPW-T	7.2791	8.4448	9.6149	11.0912	12.7325	14.8018	18.4163	41.4327

TABLE VI
REQUIRED $P_{T,d}^{(m)}$ VALUES (IN dB) FOR DIFFERENT ALGORITHMS: $G = 16$, $c_d = 0.6$, TYPE 2

User No.	8	9	10	11	12	13	14	15
D-MMSE	8.6641	10.1422	14.5733	14.7733	18.4413	-	-	-
FC-MMSE	7.8775	9.2867	10.7135	12.5124	15.1815	22.4250	-	-
NC-MMSE	8.5225	9.9611	11.7108	14.3826	17.5736	-	-	-
D-MRC	8.9023	10.4710	12.6439	17.0494	33.0294	-	-	-
FC-MRC	8.0325	9.3985	11.2078	14.1097	17.9302	-	-	-
NC-MRC	8.7545	10.2983	12.6029	16.3568	31.2467	-	-	-
IVPW-1	7.7633	9.1026	10.4319	12.1859	14.2236	17.3542	25.0579	-
VPW-1	7.7808	9.1150	10.4669	12.1804	14.4892	17.6328	28.1726	-
IVPW-A	7.7623	9.1284	10.5998	12.0950	14.1658	17.2226	24.5724	-
IVPW-T	7.7114	9.0375	10.3434	11.9926	13.9699	16.8943	23.0094	-

where

$$\mathbf{p}_u^{(m)} = [P_{u,1}^{(m)}T/N_0, \ldots, P_{u,N}^{(m)}T/N_0]^T$$

$$\mathbf{g}_u^{(m)} = \left[((c_u P_{T,u}^{(m)}/G + 1)\|\mathbf{w}_{u,1}\|^2)/(\sum_{l=1}^{L_1} |\mathbf{w}_{u,1}^H \mathbf{h}_{u,1}^{(l)}|^2), \ldots \right.$$
$$\left. ((c_u P_{T,u}^{(m)}/G + 1)\|\mathbf{w}_{u,N}\|^2)/(\sum_{l=1}^{L_N} |\mathbf{w}_{u,N}^H \mathbf{h}_{u,N}^{(l)}|^2)\right]^T.$$

The average intracell interference power can be computed by

$$P_{T,u}^{(m)} = E\left[\mathbf{1}^T \mathbf{R}_u \mathbf{p}_u^{(m)}\right] \tag{22}$$

Direct calculation of (22) yields $P_{T,u}^{(m)} = ((c_u P_{T,u}^{(m)})/(G) + 1)P_{T,u}^{(s)}$ or (11).

B. Intracell Interference for Downlink Multiple-Cell Environment

If same number of users is considered for both single- and multiple-cell cases, the power control problem is given by

$$\left(\mathbf{I} - \gamma_d \mathbf{F}_d^{(s)}\right)\mathbf{p}_d^{(m)} = \gamma_d \mathbf{g}_d^{(m)} \tag{23}$$

where

$$\mathbf{p}_d^{(m)} = [R^{-\alpha}P_{d,1}^{(m)}T/N_0, \ldots, R^{-\alpha}P_{d,N}^{(m)}T/N_0]^T$$

$$\mathbf{g}_d^{(m)} = \left[(v_1 P_{T,d}^{(m)}/G + (d_1/R)^\alpha)/(\sum_{l=1}^{L_1} |\mathbf{w}_{d,1}^H \mathbf{h}_{d,1}^{(l)}|^2), \ldots \right.$$
$$\left. (v_N P_{T,d}^{(m)}/G + (d_N/R)^\alpha)/(\sum_{l=1}^{L_N} |\mathbf{w}_{d,N}^H \mathbf{h}_{d,N}^{(l)}|^2)\right]^T.$$

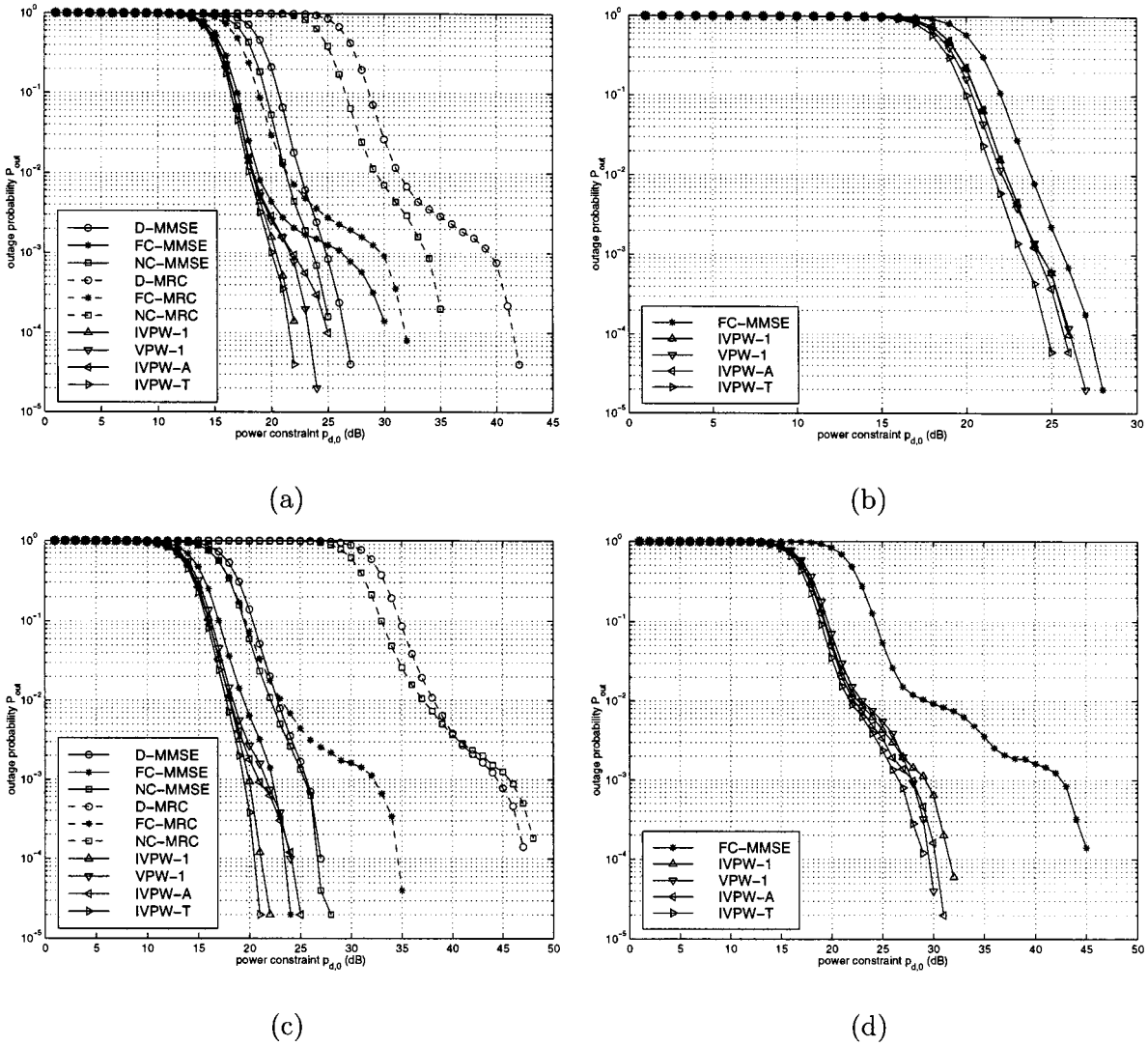

Fig. 6. Multicell outage probability for different algorithms with respect to power constraint. (a) Type 1, $N = 13$. (b) Type 1, $N = 14$. (c) Type 2, $N = 12$. (d) Type 2, $N = 13$.

TABLE VII
MULTI-CELL CAPACITY FOR DIFFERENT ALGORITHMS WITH DIFFERENT POWER CONSTRAINTS, $P_{d,0}$'s: $G = 16$, $c_d = 0.6$

$P_{d,0}$	20dB	30dB	40dB	∞	20dB	30dB	40dB	∞
Traffic	Type 1	Type 1	Type 1	Type 1	Type 2	Type 2	Type 2	Type 2
D-MMSE	12	13	13	13	11	12	12	12
FC-MMSE	13	14	14	14	12	13	13	13
NC-MMSE	12	13	13	13	11	12	12	12
D-MRC	10	12	13	13	10	11	12	12
FC-MRC	12	13	13	13	11	12	12	12
NC-MRC	12	13	13	13	10	11	12	12
IVPW-1	13	14	14	14	12	14	14	14
VPW-1	13	14	14	14	12	13	14	14
IVPW-A	13	14	14	14	12	14	14	14
VPW-T	13	14	14	15	12	14	14	14

The average intra-cell interference power can be computed by,

$$P_{T,d}^{(m)} = E\left[\mathbf{1}^T \mathbf{R}_d \mathbf{p}_d^{(m)}\right] \tag{24}$$

which yields $P_{T,d}^{(m)} = (\gamma_d G E_r \bar{\mu}_d^{(s)})/(G - \gamma_d c_d \bar{\mu}_d^{(s)})$, thus (15) from (14), where $c_d = E[v_k]$.

REFERENCES

[1] A. F. Naguib, A. Paulraj, and T. Kailath, "Capacity improvement with base-station antenna arrays in cellular CDMA," *IEEE Trans. Veh. Technol.*, vol. 43, pp. 691–698, Aug. 1994.

[2] F. Rashid-Farrokhi, L. Tassiulas, and K. J. R. Liu, "Joint optimal power control and beamforming in wireless networks using antenna arrays," *IEEE Trans. Commun.*, vol. 46, pp. 1313–1324, Oct. 1998.

[3] S. Tanaka, M. Sawahashi, and F. Adachi, "Pilot symbol-assisted decision-directed coherent adaptive array diversity for DS-CDMA mobile radio reverse link," *IEICE Trans. Fundamentals*, vol. E80-A, no. 12, pp. 2445–2553, Dec. 1997.

[4] F. Rashid-Farrokhi, K. J. R. Liu, and L. Tassiulas, "Transmit beamforming and power control for cellular wireless systems," *IEEE J. Select. Areas Commun.*, vol. 16, pp. 1437–1449, Oct. 1998.

[5] H. Suda, F. Kikuchi, and F. Adachi, "Effect of fast transmit power control on DS-CDMA forward link capacity," in *Proc. Asia Pacific Conf. Communications/Singaporte Int. Conf. Communication Systems*, Singapore, Nov. 1998, pp. 413–417.

[6] U. Forssen *et al.*, "Method of and Apparatus for Interference Rejection Combining and Downlink Beamforming in a Cellular Radiocommunications System,", May 27, 1997. filed.

[7] F. Adachi, "Effects of orthogonal spreading and Rake combining on DS-CDMA forward link in mobile radio," *IEICE Trans. Commun.*, vol. E80-B, no. 11, pp. 1703–1712, Nov. 1997.

[8] P. Newson and M. R. Heath, "The capacity of a spread spectrum CDMA system for cellular mobile radio with consideration of system imperfections," *IEEE J. Select. Areas Commun.*, vol. 12, pp. 673–683, May 1994.

[9] A. J. Viterbi and A. M. Viterbi, "Other-cell interference in cellular power-controlled CDMA," *IEEE Trans. Commun.*, vol. 42, pp. 1501–1504, Feb. 1994.

[10] Y.-C. Liang and F. Chin, "Effect of power constraint on uplink capacity of DS-CDMA systems with antenna array and SIR-based power control," presented at the Conf. Personal, Indoor, Mobile Radio Communications, Osaka, Japan, Sept. 1999.

[11] Y.-C. Liang, F. Chin, and K. J. R. Liu, "Downlink beamforming for DS-CDMA mobile radio with multimedia services," in *Proc. Vehicular Technology Conf.*, Amsterdam, The Netherlands, Sept. 1999, pp. 17–21.

[12] Y.-C. Liang and F. Chin, "Downlink channel covariance matrix (DCCM) estimation and its applications in wireless DS-CDMA systems," *IEEE J. Select. Areas Commun.*, vol. 19, Feb. 2001.

[13] R. Steel, *Mobile Radio Communications.* New York: IEEE Press, 1992.

[14] C. Farsakh and J. A. Nossek, "Spatial covariance based downlink beamforming in an SDMA mobile radio system," *IEEE Trans. Commun.*, vol. 46, pp. 1497–1506, Nov. 1998.

[15] Y.-C. Liang, F. Chin, and K. J. R. Liu, "Downlink beamforming for DS-CDMA mobile radio with multimedia services," *IEEE Trans. Commun.*, vol. 49, July 2001.

[16] G. Xu and H. Liu, "An efficient transmission beamforming scheme for frequency-division-duplex digital wireless communications systems," in *Proc. Int. Conf. Acoustics, Speech and Signal Processing*, Detroit, MI, May 1995, pp. 1729–1732.

[17] D. Gerlach and A. Paulraj, "Adaptive transmitting antenna arrays with feedback," *IEEE Signal Processing Lett.*, vol. 1, pp. 150–152, Oct. 1994.

[18] G. G. Raleigh and A. Paulraj, "Adaptive transmitting antenna methods for multipath environmemts," in *Proc. Globecom*, San Francisco, CA, Nov. 1994, pp. 425–429.

[19] G. G. Raleigh, S. N. Diggavi, V. K. Jones, and A. Paulraj, "A blind adaptive transmit antenna algorithm for wireless communications," in *Proc. Int. Conf. Communications*, Seattle, WA, June 1995, pp. 1494–1499.

[20] G. G. Raleigh and V. K. Jones, "Adaptive antenna transmission for frequency duplex digital wireless communication," in *Proc. Int. Conf. Communications*, Montreal, QC, Canada, June 1997, pp. 641–646.

Ying-Chang Liang (M'00–SM'01) received the B.S. and Ph.D. degrees in electrical engineering from Jilin University of Technology, Changchun, China, in 1989 and 1993, respectively. He did post-doctoral research at Tsinghua University, China, and Nanyang Technological University, Singapore, between 1994 and 1996.

In 1997, he was a Research Associate with the Electrical Engineering Department, University of Maryland, College Park, where he conducted research on transmit diversity for IS-136 TDMA systems, closely with AT&T Labs—Research. He joined the Centre for Wireless Communications (CWC), Singapore in 1997, where he currently is a Senior Member of Technical Staff in the Communication Systems and Signal Processing Group. In CWC, he participated in a joint project between CWC and NTT DoCoMo, designing a smart antenna system for wideband CDMA. His research interests include adaptive signal processing for wireless communications, statistical signal processing, and higher order statistics.

Dr. Liang received the Best Paper Award from the 50th IEEE Vehicular Technology Conference—(IEEE VTC'99-Fall). He was also the co-receipient of 1997 National Natural Science Award and 1996 Science and Technology Achievement Award, both from China. Dr. Liang holds five pending patents.

Francois Chin received the Ph.D. degree in electrical engineering from National University of Singapore in 1996.

Since September 1995, he has been with the Centre for Wireless Communications, a government-funded research centre linked to NUS, when he is now a Senior Member of Technical Staff and leads a R&D team in future broadband wireless access. His research interests include signal processing techniques for capacity/quality enhancement and communication system design/performance evaluation.

Dr. Chin is a co-recipient of IEEE Vehicular Technology and Communications Conference (1999-Fall in Amsterdam) Best Paper Award.